ARTICLE

B. Lehmann · J. Heinhorst · U. Hein · M. Neumann
J. D. Weisser · V. Fedesejev

The Bereznjakovskoje gold trend, southern Urals, Russia

Abstract The East Uralian Zone south of Cheljabinsk consists of a Silurian to Early Carboniferous volcano-sedimentary sequence on Proterozoic basement, intruded by postorogenic Permian granitic rocks. The 7 by 1–2 km Bereznjakovskoje gold trend is hosted by dacitic to andesitic volcanic-subvolcanic units of Late Devonian age. Epithermal gold mineralization is of the sulfide-rich low-sulfidation (adularia-sericite) type with the metal spectrum of Au-Ag-As-Sb-Cu-Zn-Pb and a characteristic Te component. Silicic and sericitic alteration overprints barren propylitic pyrite-rich assemblages in stockworks and shear zones. Precious-metal mineralization is related to a fahlore-telluride stage overprinting earlier pyrite. Late stage redistribution and weathering liberates gold from telluride mineral phases with fixation of native gold (high fineness) on vugs and grain boundaries, and in intergrowth aggregates with supergene jarosite/limonite. Epithermal mineralization formed below the boiling level and is possibly related to a porphyry system at depth.

Introduction and geologic setting

Gold mining started in the Ural Mountains 250 years ago with about 400 t gold produced to date (EMJ 1996). Most of this production is from placers and some me-

B. Lehmann (✉) · J. Heinhorst · U. Hein
Institut für Mineralogie und Mineralische Rohstoffe,
Technische Universität Clausthal, Adolph-Roemer-Str. 2A,
D-38678 Clausthal-Zellerfeld,
Germany

M. Neumann · J.D. Weisser
Sachtleben Bergbau Services GmbH, PO Box 70 05,
D-57358 Lennestadt,
Germany

V. Fedesejev
Roskomnedra, Blukhera Street 8A, Cheljabinsk, 454048 Russia

sothermal gold-quartz-sulfide systems. Both historically and at present, placers contribute about 70% of the total gold production of Russia (Benevolski 1995). Exploration for epithermal deposits started only recently, revealing a hitherto neglected potential for epithermal gold in the Urals.

The Uralide orogen developed through the assembly of rifted microcontinental fragments and Paleozoic island-arc and back-arc basins of the Uralian paleo-ocean. The final collision of this complex accretionary collage with the East European craton (Baltica) to the west, and the Siberian craton to the east took place in Late Carboniferous and Permian time (Zonenshain et al. 1984; Berzin et al. 1996). Lower Paleozoic oceanic crust is preserved only within sutures in between major belt-like slices/megablocks of volcanic arc and continental rock associations.

The area south of Cheljabinsk is part of the low-gravity East Uralian zone composed of a metamorphic basement (granite-gneiss domes) with Lower Paleozoic schist envelopes, known as the Pre-Uralides (Zonenshain et al. 1984). The Pre-Uralides are overlain by an Upper Devonian to Lower Carboniferous volcanosedimentary calc-alkaline sequence of a late island arc environment. The Upper Paleozoic sequence is characterized by dacitic to andesitic magmatism with extensive welded tuff occurrences and coeval minor porphyritic intrusions. Some porphyry intrusions have low-grade Cu-Au-Mo stockwork mineralization (Grabezhev et al. 1995). Major syn-/post-collisional granite intrusions are of Upper Carboniferous-Permian age and host gold-bearing mesothermal quartz-sulfide shear zones with propylitic alteration.

The southern Urals have a present-day crustal thickness of 50–60 km and apparently experienced little or no postorogenic collapse. This region probably never developed into a gravitationally unstable belt of high mountains as is found in most modern continental collisions (Berzin et al. 1996) which could account for the preservation of shallow volcanic features of the Upper Paleozoic magmatic arc, including epithermal systems.

The regional geologic setting of the study area, with emphasis on gold mineralization, is shown in Fig. 1. North-northeast trending slices of continental crust (Precambrian basement plus Lower Paleozoic volcanic arcs) are enclosed by sheared suture zones with Lower Paleozoic ophiolites. The Karabash-Miass shear zone to the west is part of the Main Uralian Fault/suture zone and hosts a number of large Cu-Zn-Au massive sulfide deposits. There are a number of poorly defined gold-bearing copper porphyry systems, and there are a multitude of vein-type gold systems from the epithermal-mesothermal spectrum. The Kochkar Mine at Plast (Uralzoloto), currently on standby, was the most important gold producer in the region, producing from a quartz vein system with a grade of 3.5 g Au/t. The available documentation is not sufficient to draw any metallogenic conclusions.

The Bereznjakovskoje area was studied in recent years by the Geological Survey of the Cheljabinsk Oblast (Roskomnedra) in cooperation with western joint venture partners. The main exploration tool was geochemistry. Extensive soil sampling, trenching and shallow reconnaissance drilling, as well as detailed exploration drilling to a depth of up to 400 m, identified centres of gold mineralization along a 7 by 1–2 km alteration and mineralization trend striking north-south, the Bereznjakovskoje gold trend. The total gold potential is estimated at 50–100 t Au. Only one center has been explored in detail and has drill-indicated geological ore reserves of about 20 t gold at > 3g/t Au. Exploration and definition drilling is currently going on.
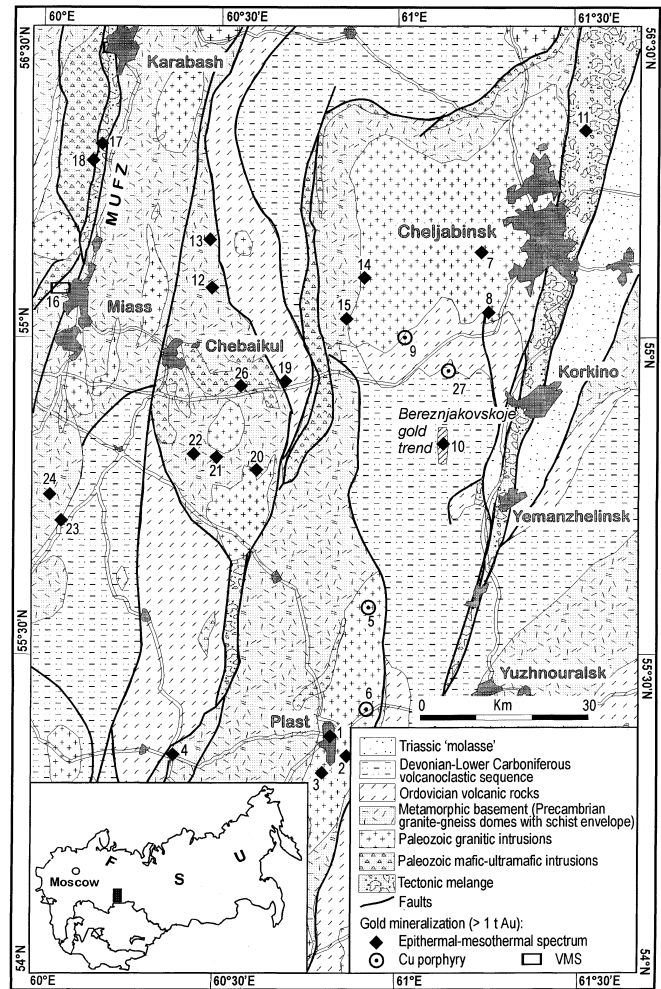
Igneous petrology and hydrothermal alteration

The study area is in flat-lying terrain with several meters of soil cover, and all petrologic information is from drillcore material. The bedrock is a dacite to andesite volcanoplutonic sequence with a regional propylitic overprint. Gold mineralization occurs in m- to dm-scale structurally controlled zones of silicification with sericite/muscovite alteration haloes.

The most prevalent rock type is composed of medium-grained, corroded quartz phenocrysts, angular feldspar fragments, and relics of phyllosilicates set in a very fine-grained quartz-sericite/illite matrix. A relict volcanoclastic fabric is often displayed by sericite/illite intergrowth aggregates with angular outlines of former glass shards. Some rock portions have a porphyritic fabric with corroded quartz and subhedral feldspar phenocrysts (largely replaced by carbonate) suggestive of subvolcanic intrusive stocks. Cross-cutting monzonite dykes have seriate to equigranular fabric composed of abundant hypidiomorphic plagioclase and granoblastic quartz, and are characterized by albitization, silicification and carbonate blastesis.

The discrimination diagrams of Fig. 2 show the volcanic-arc nature of these rocks and their location in the andesitic to dacitic compositional field, with dacitic samples characterized by weak silicic overprint.

The pyroclastic wall rocks of the Bereznjakovskoje system are pervasively altered to propylitic mineral assemblages (probably a regional overprint). Alteration zones around mineralized quartz lenses/shear zones consist mainly of silicic and sericitic assemblages with subordinate adularia and locally argillic alteration (Fig. 3A). Major gangue components of the hydrothermal system are quartz-sericite/muscovite-calcite. Minor amounts of adularia rhombs and barite, and the absence of advanced argillic alteration, indicate that the sulfide/telluride quartz vein mineralization is comparable with epithermal deposits of adularia-sericite or low-sulfidation type (Heald et al. 1987).

Silica is mostly in the form of fine-grained comb quartz/ribbon quartz and interlocking lenticular quartz mosaics within networks of veinlets with deformation-related superimposed textures. Flamboyant quartz textures around pyrite idioblasts suggest recrystallization of amorphous silica (Dong et al. 1995) (Fig. 3B). Crustiform and colloform textures are subordinate; bladed textures and chalcedony were not observed. The quartz textures suggest an environment characteristic of the

Fig. 1 Generalized geological map of part of the SE Urals (compiled from Geological map of Cheljabinsk ore area 1:500 000, VSEGEI St. Petersburg, unpubl.; gold mineralization of the southern Urals 1:200 000, VSEGEI St. Petersburg, unpubl.). *MUFZ*, Main Uralian Fault Zone. Gold mineralization:

1	Kochkarskoje	LD	1 (Au-Ag-As-Te-Bi)
2	Novotroitskoje	MD	1 (Au-Ag-As-Te-Bi)
3	Oseiskoje Levoberazhie	SD	1 (Au-Ag-As-Te-Bi)
4	Svetlinskoje	LD	1 (Au-Ag-Cu-Te)
5	Zeleny Dol	SD	2 (Cu-Mo-Au)
6	Polyanovskoje	SD	2 (Cu-Mo-Au)
7	Shershnevskoje	SD	1 (Au-As-W)
8	Udaly Priisk	SD	1 (Au-As)
9	Birgildinskoje	SD	2 (Cu-Mo-Au)
10	Bereznjakovskoje	LD	1 (Au-Ag-Cu-As-Te)
11	Prokhorvskoje	SD	1 (Au)
12	Nepryakhinskoje	SD	1 (Au-Ag-Cu-As-Pb-Zn)
13	Maiskoje	SD	1 (Au-Ag-Cu-As-Pb-Zn)
14	Narybakovskoje	SD	1 (Au-As-W-Mo)
15	Adzhitarovskoje	SD	1 (W-Au-As)
16	Melentievskoje	MD	3 (Cu-Pb-Zn-Au-Ag)
17	Nailinskoje	SD	1 (Au)
18	Tyelginskoje	SD	1 (Au-Cu-Pb)
19	Melnikovo-Zauralskoje	SD	1 (Au-W-Cu)
20	Vladimirskoje	SD	1 (Au-Cu-Pb-Zn)
21	Kazantsevskoje	SD	1 (Au-Ag-Cu-Pb-Zn-As)
22	Bolshakovskoje	SD	1 (Au-Ag-Cu-Pb-Zn-As)
23	Kolpakovskoje	SD	1 (Cu-Au)
24	Chistogorskoje	SD	1 (Au-Ag-Cu-W)
25	Dzerzhinskoje	MD	3 (Cu-Au-Ag)
26	Khadpevskoje	SD	1 (Au-Ag-Cu-Pb-Zn-As)
27	Tominskoje	SD	2 (Cu-Mo-Au)

SD, 1–10 t Au
MD, 10–50 t Au
LD, 50–100 t Au

1, epithermal-mesothermal vein spectrum
2, porphyry
3, massive sulfide deposit

deeper parts of epithermal veins below the boiling level (Dowling and Morrison 1989).

Structure

Brecciation, silicification and quartz-sulfide veining define east-west striking irregular lens-like bodies several meters wide and up to 200 m long. These lenses with a 40–70° dip to the north appear to be extensional fractures and shear zones, probably part of a northwest-oriented sinistral strike-slip regime in a regional east-west oriented compressional stress field (Pushakov and Kuznezov 1995). The extensional fractures occur in *en echelon* spacing and display complex internal deformation fabrics with repeated hydrothermal precipitation and fracturing episodes which led to a variety of quartz recrystallization fabrics from fine-grained ribbon quartz and quartz mosaics to shear-controlled comb spider veinlets.

Strike-slip faulting with repeated reversal of shear sense in between Baltica and Siberia is the dominant tectonic feature of the orogenic evolution of the Uralides (Sengör et al. 1993). As a result, local transpressional and transtensional domains can act as discharge for overpressured fluids in the general compressive regime. These local domains consist of a mesh of minor faults and extensional fractures, and can repeatedly become reactivated by fluid pressure cycling (Sibson 1996). Such a fault-valve process of multiple episodes of rupturing, fluid flow and hydrothermal sealing is probably seen in the complex internal quartz deformation fabrics. The several kilometer in size and defocused fluid system in the Bereznjakovskoje gold trend gives this area a large ore potential.

Mineralization

The Bereznjakovskoje gold trend is characterized by a 7 km long north-south trending zone with a number of ore centers which are locally controlled by northwest and east-west striking secondary shear zones. Structurally controlled silicification and sericite/muscovite alteration halos define the ore systems on a meter to 10-m scale. Gold mineralization occurs in north-west and east-west trending vein sets and multidirectional veinlets/stockworks in association with pyrite, fahlore and tellurides (refractory gold). The uppermost 30–40 m below the surface are weathered and the oxidized material carries free gold in association with limonite and jarosite. At > 300 m depth, the system has abundant disseminated and stockwork pyrite mineralization, which is mostly barren.

The mineralization was studied in about 60 polished sections by reflected light microscopy. Ore microscopy was accompanied by electron microprobe analysis, using the energy dispersive subsystem of a Cameca SX 100.
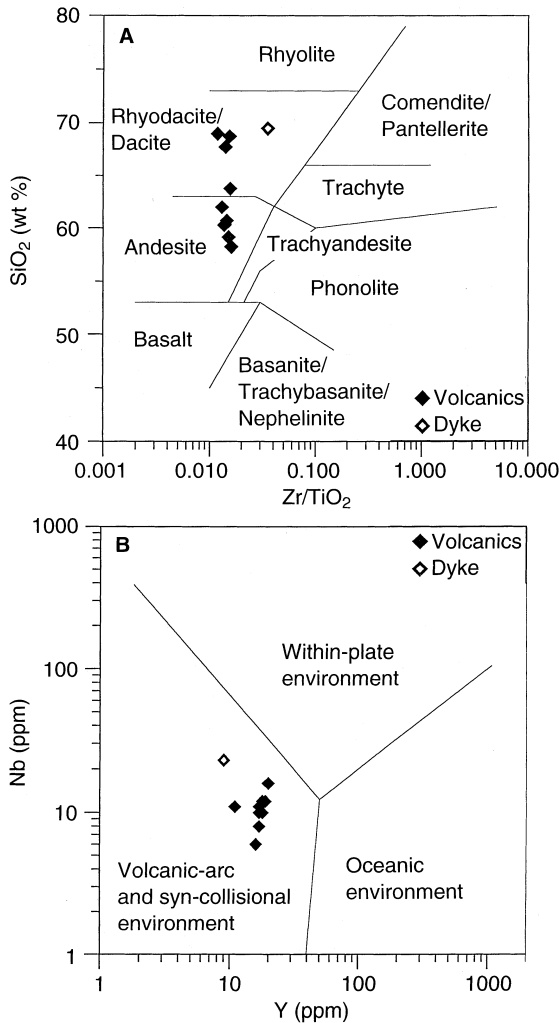
Fig. 2 A Hydrothermally altered igneous rocks from Bereznjakovskoje in the SiO_2-Zr/TiO_2 discrimination diagram of Winchester and Floyd (1977); **B** the same samples in the Nb/Y geotectonic discrimination diagram of Pearce et al. (1984)

Textural relationships allow grouping of ore mineralization into three temporal stages:

1. The early pyrite stage occurs both as pervasive impregnations of wall rocks and brecciated vein filling within silicified wall rocks over a large depth interval of >300 m. Pyrite mineralization is very prominent and increases towards depth as part of a propylitic mineral association (quartz-carbonate-chlorite-sericite-epidote-rutile-pyrite). Coarse-grained pyrite is often zoned and has small inclusions of pyrrhotite and chalcopyrite.

2. The subsequent polymetallic stage is represented by veinlet mineralization with fahlore as the dominant ore component. Fahlore (mostly high-Cu tennantite, minor tetrahedrite) corrodes the earlier pyrite and fills spaces in porous pyrite aggregates (Fig. 3C). Cu:Zn:Fe atomic ratios in fahlore are around 12:2:0.8. Silver contents vary from <0.1 wt.% to 0.65 wt.%. Low-Fe sphalerite (<0.4 wt.% Fe) oc-

Fig. 3 A Rhombic adularia prophyroblasts (*center*; distinct relief) in quartz-sericite matrix. Opaque minerals are pyrite and fahlore. Sample 226/139.5 m, thin section, plane polarized light, 100×. **B** Silicic and pyrite alteration: subhedral pyrite blasts enclosed by flamboyant-textured quartz aggregates in fine-grained quartz-sericite/illite groundmass. Sample C4B/131.5 m, thin section, crossed nicols, 25×. **C** Zoned pyrite aggregates corroded by fahlore (*medium gray*) and quartz (*black*). Sample 226/139.5 m, polished section, plane polarized light, air, 50×. **D** Zoned pyrite aggregate corroded by fahlore. Small intergrowth aggregates of petzite (*medium gray*) and calaverite (*white*; lighter than pyrite) with very small gold aggregates on petzite-pyrite grain boundaries. Sample 224/58.6 m, polished section, plane polarized light, oil immersion, 500×. **E** Porous pyrite aggregates corroded by fahlore (*dark gray*) and quartz (*black*). Pyrite hosts amoeboid inclusions of altaite (*white*) and clausthalite (*light gray*). Sample 208/273 m, polished section, plane polarized light, oil immersion, 500×. **F** Altaite with intergrowth lamellae of both tellurobismuthite (*pinkish*) and gold in fahlore. Gold also on vugs (*black*). Sample C0B/95.5 m, polished section, plane polarized light, oil immersion, 1000×. **G** Brecciated fahlore (*dark gray*) with intergrowth aggregate of petzite (*gray*), altaite (*white*), and amoeboidal gold. Sample C0B/95.5 m, polished section, plane polarized light, oil immersion, 1000×. **H** Intergrowth aggregate of altaite (soft; *light gray*), petzite (*medium gray*) and gold (mostly on rims around altaite). Matrix is quartz (*black*) and fahlore (*dark gray*) Sample C0B/95.5 m, polished section, plane polarized light, oil immersion, 1000×

curs together with fahlore, locally replacing fahlore. A number of tellurides are associated with fahlore mineralization (Figs. 3D–H). The most abundant telluride is altaite (PbTe; white, very high reflectivity, large aggregates up to mm-size), followed by petzite (Ag_3AuTe_2; violet color, medium reflectivity). The ratio of abundance of altaite to petzite is about 10. Altaite is occasionally intergrown with rare clausthalite (PbSe,S), galena, and tellurobismuthite (Bi_2Te_3; lamellae in altaite). Less abundant tellurides are: calaverite ($AuTe_2$, white-cream, high reflectivity), hessite (Ag_2Te; brownish-violet, medium reflectivity), sylvanite ($AuAgTe_4$; yellow-white, high reflectivity), weissite (Cu_2Te; bluish secondary color, low reflectivity), coloradoite (HgTe; pink, medium to high reflectivity), and kostovite ($CuAuTe_4$; yellow, medium to high reflectivity). All tellurides occur as late phases on cracks and in vugs of pyrite in fahlore, but also intergrown with fahlore, pointing to a late tellurium-, precious- and base metal-rich fluid (Figs. 3D–H). Gold is occasionally intergrown with altaite and petzite (Figs. 3F and G).

3. Most native gold occurs on cracks and open spaces in fahlore and pyrite. The gold aggregates are mostly in the μm size range and have very little Ag (<10wt.% Ag). Some of the native gold is intergrown with, or forms rims on, argentite, petzite and weissite (Figs. 3 F–H). Most native gold is located on grain boundaries and occurs controlled by secondary permeability together with limonite and jarosite which suggests an origin by supergene processes, i.e., weathering of tellurides.

The often seen calaverite-petzite-gold intergrowth textures with the abundance of altaite define a relatively
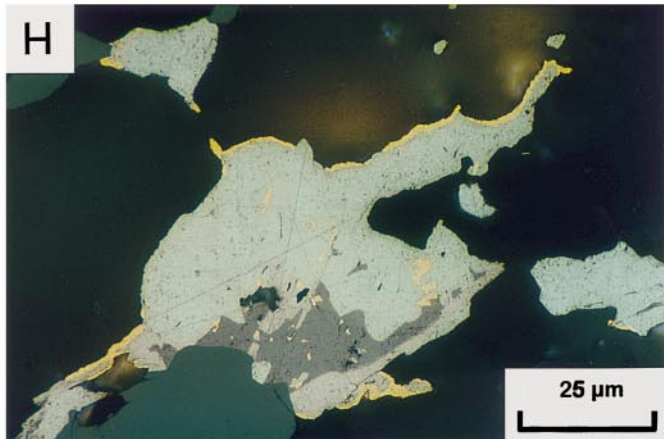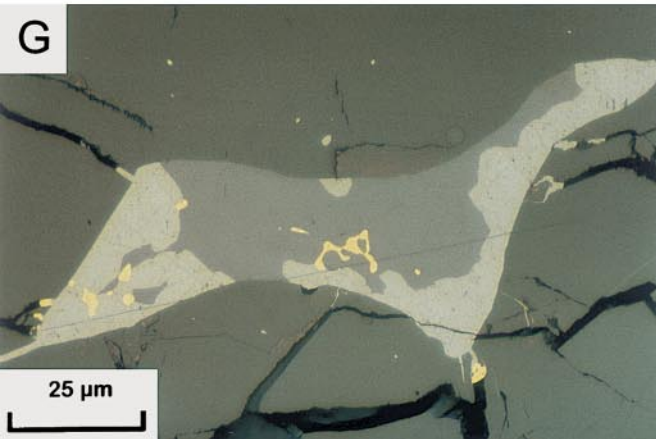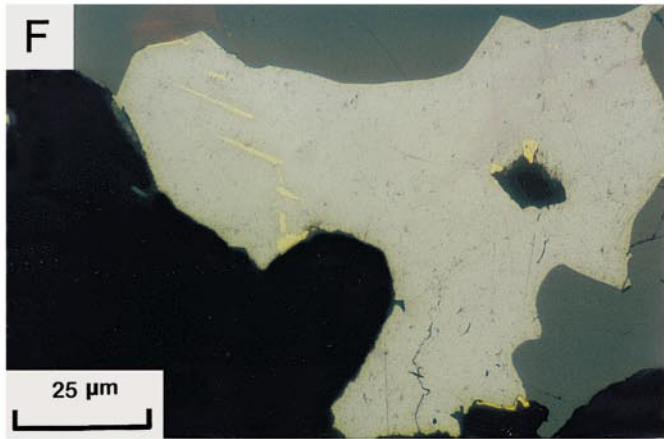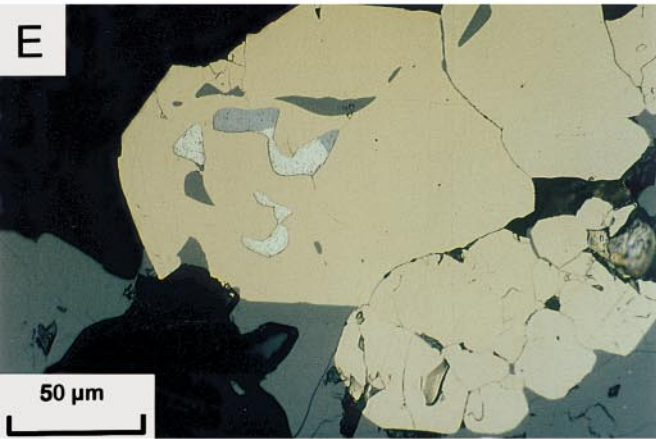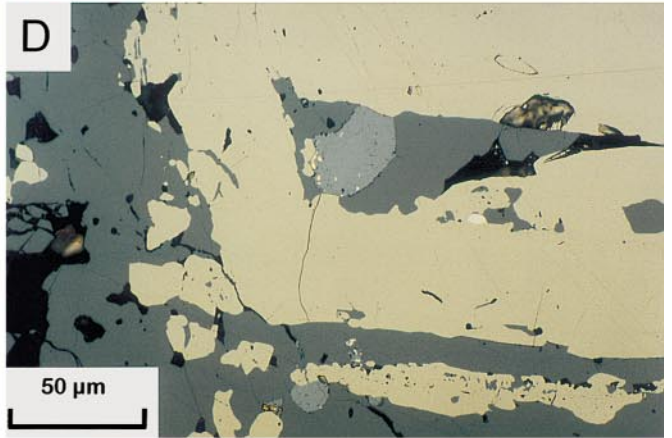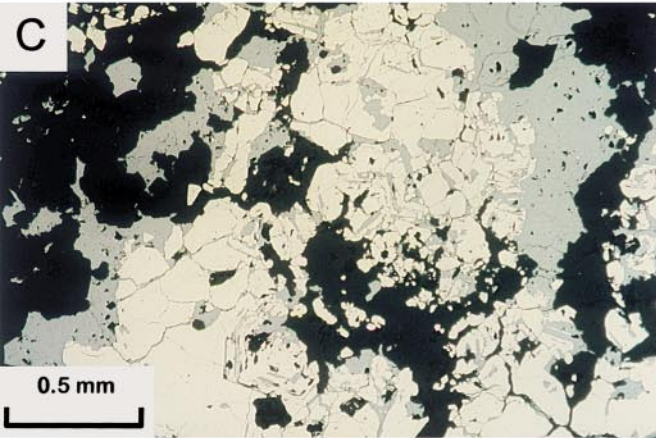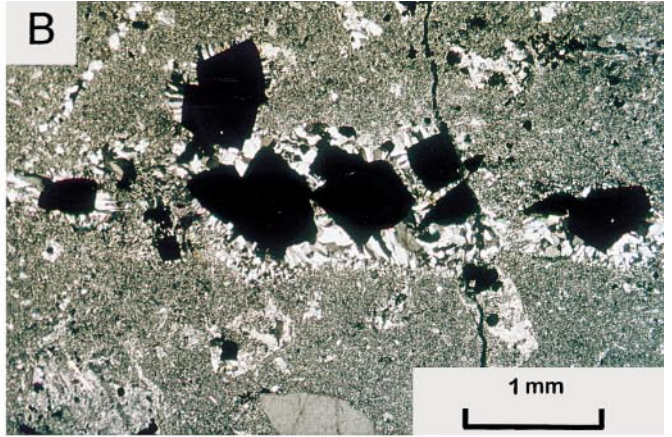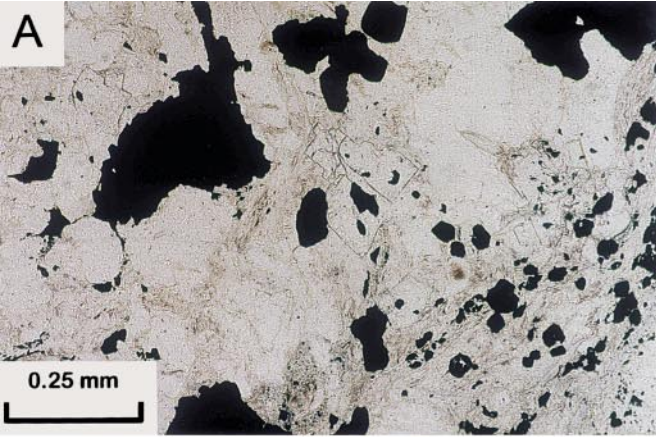
restricted high-Te/low-S compositional space of the ore system during the fahlore/telluride stage, and primary gold fixation suggestive of a short-lived (magmatic?) Te and Au input (Fig. 4). This relationship holds true for the central parts of the hydrothermal systems. Peripheral parts are characterized by much lower abundance of tellurides and lower gold values, with galena instead of altaite. This relationship indicates much less Te in the periphery of the systems, with f_{Te} below the alatite-galena equilibrium (Fig. 4).

Fluid inclusions

Reconnaissance fluid inclusion petrography could not find measurable primary fluid inclusions within hydrothermal ore-related quartz. However, secondary two-phase aqueous fluid inclusions in magmatic quartz phenocrysts of the host rock are associated with carbonate, sericite and sulfide particles on microfractures. These particles also occur occasionally as solid phases within the fluid inclusions. Initial melting temperatures of > -21 °C indicate dominance of NaCl. Ice melting is the only phase transition observable at low temperatures. Final melting temperatures are −6 to −2 °C, which represent salinities of about 3–8 equivalent wt.% NaCl. The two-phase inclusions homogenize into the liquid phase in a temperature range of 130–220 °C; most have homogenization temperatures in between 145–185 °C (Fig. 5). Evidence for boiling was not observed.

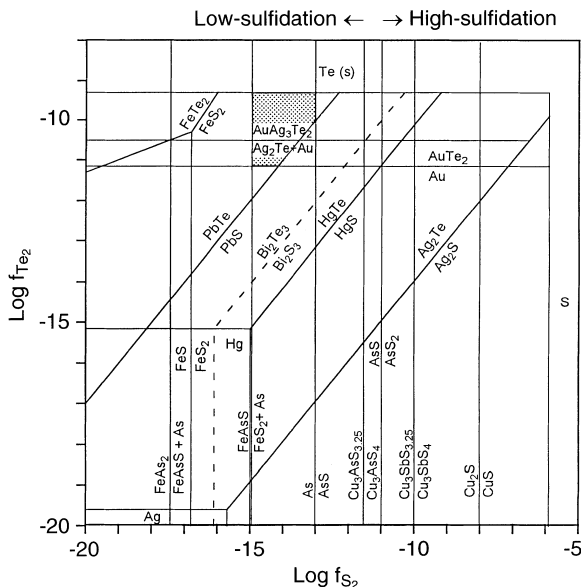A second population of fluid inclusions occurs in hydrothermal quartz veinlets cross-cutting sericite-car-

Fig. 5 Salinity-homogenization temperature variation diagram for fluid inclusions of the Bereznjakovskoje ore system. Ore stage is defined by secondary fluid inclusion trails (co-genetic with sericite-carbonate-sulfides) in host rock quartz phenocrysts, post ore stage by primary fluid inclusions in hydrothermal quartz

bonate-sulfide altered rocks. This post-ore hydrothermal quartz is occasionally zoned and contains primary two-phase fluid inclusions. The fluid inclusions homogenize into the liquid phase at temperatures of 80–105 °C; their salinity is ≤1 equivalent wt.% NaCl ($Tm_{ice} > -0.5$ °C).

The relatively restricted range of homogenization temperatures at variable salinities suggests fluid mixing during ore formation, concomitant with cooling and dilution. We do not know the pressure of the system but a realistic estimate from quartz fabrics and other geological features is in between 100 bar to 1 kbar. A pressure correction for this range would give ore-stage formation temperatures of about 170–250 °C during the fahlore-telluride mineralization stage. This is also the formation range of fine-grained rhombic adularia often seen in deep parts of epithermal systems at temperatures of < 220 °C (Dong and Morrison 1995). The earlier pyrite stage, defined by Russian workers using calcite-dolomite geothermobarometry, gave temperature and pressure intervals of 200–350 °C and 0.12–1.2 kbar, respectively (Pushakov and Kuznezov 1995). Elevated temperature for the early pyrite stage is also indicated by the occurrence of pyrrhotite-chalcopyrite inclusions in pyrite.

Trace element geochemistry

About 100 drill core samples were analyzed by Bondar Clegg, Canada, for a number of metals relevant to ex-

Fig. 4 Sulfur versus tellurium fugacity diagram with selected sulfide-telluride equilibria at 200 °C (Afifi et al. 1988; Ahmad et al. 1987; Barton and Skinner 1979). *Shaded area* locates peak gold telluride stage within the calaverite and altaite stability fields. Peripheral parts of the system are within the galena stability field
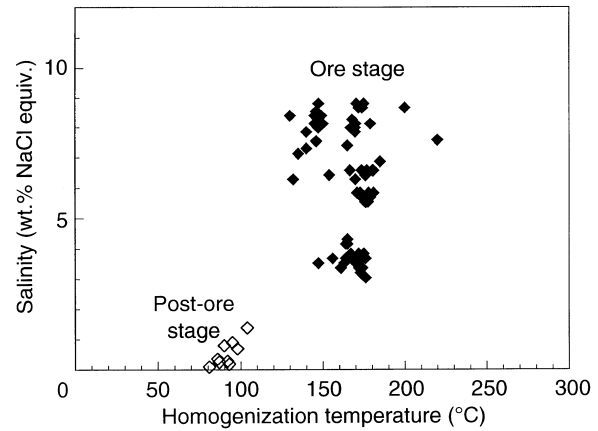
Fig. 6 Variation plots for a number of trace element pairs in whole-rock samples with primary sulfide mineralization (*solid circles*) and from the near-surface oxidation zone (*open circles*). Whole-rock samples are from drill cores of the dacitic to andesitic sequence with variable degree of mainly sericitic alteration and quartz veining. Averages of upper continental crust from Taylor and McLennan (1985) and Vinogradov (1962)
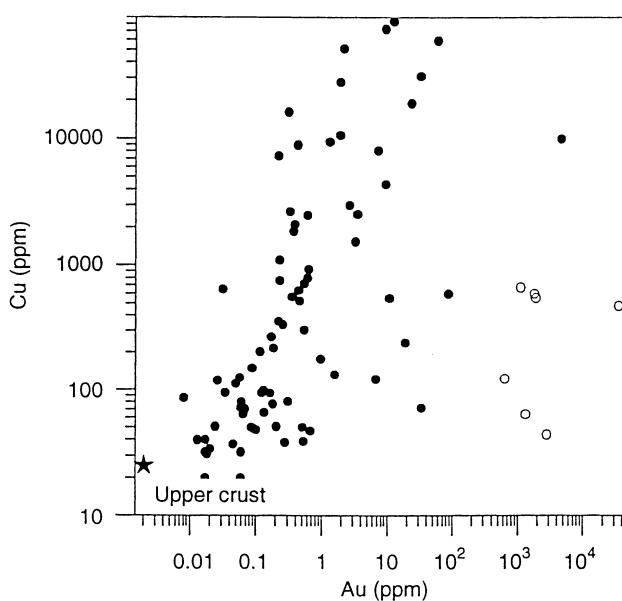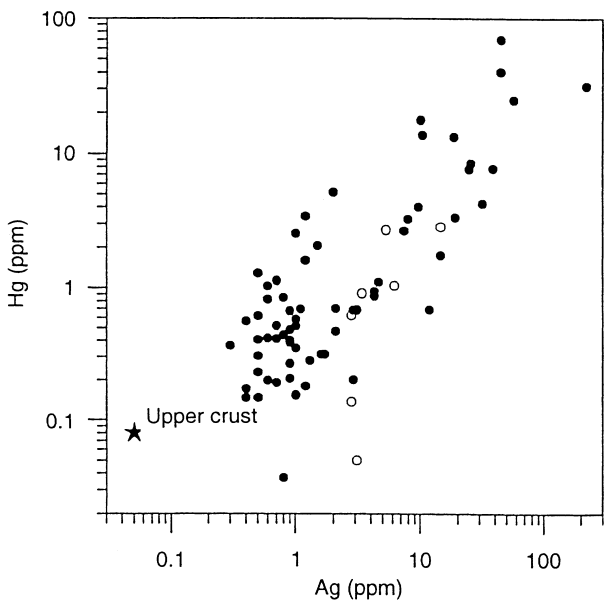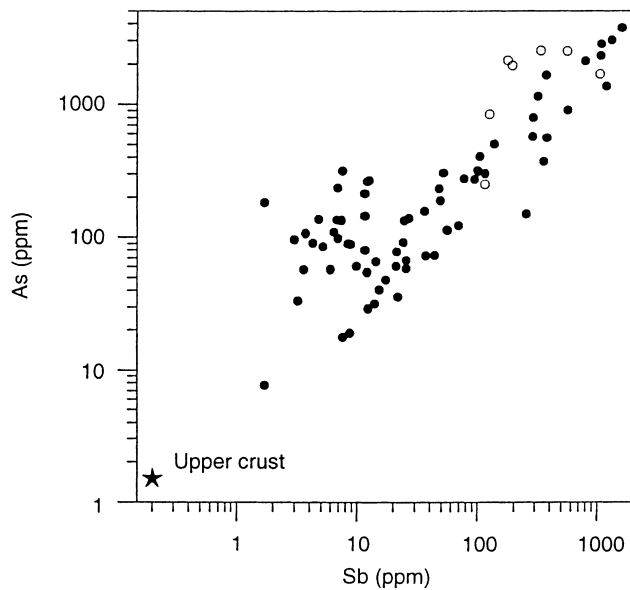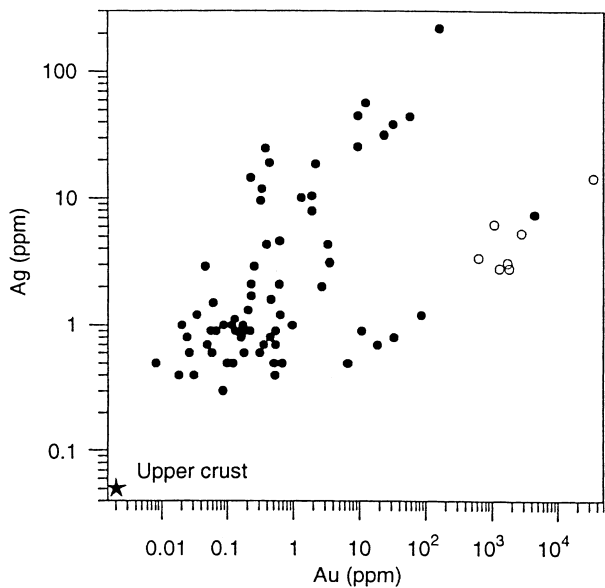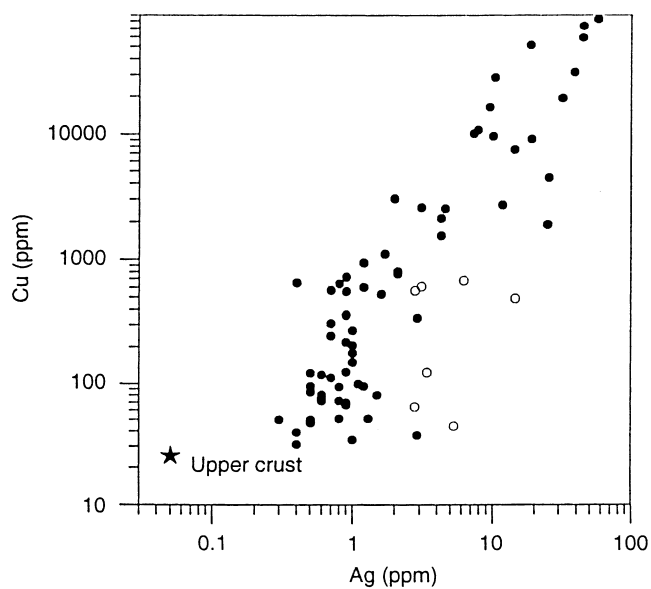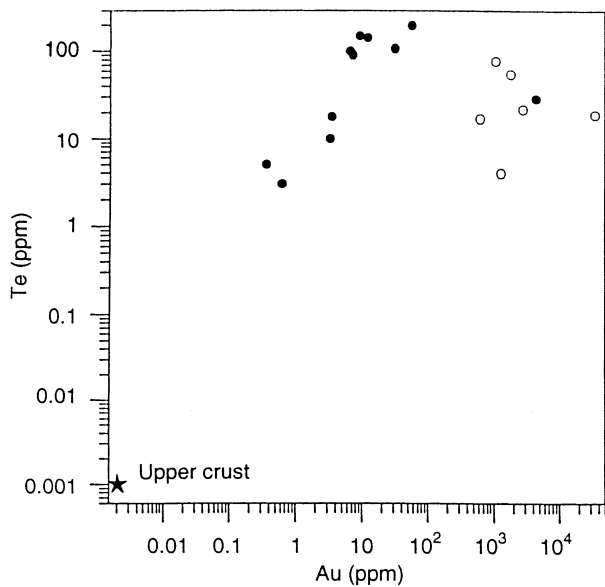
ploration. All samples are from the andesitic to dacitic volcanoplutonic sequence with variable degree of hydrothermal overprint/mineralization. Sample digestion was by aqua regia, i.e., the silicate-bound metal portions were not considered. Au and Ag were analyzed by fire assay with AAS finish, other elements by ICP and AAS with hydride technique.

The ore system is strongly enriched in the following metallic elements, compared to bulk upper continental crust (Taylor and McLennan 1985):

1. Au, As, Sb, Te ($\geq$500× upper continental crust)
2. Ag, Hg, Se, Cu (100–500× upper continental crust)
3. Zn, Bi, Pb (10–30× upper continental crust)

The average bulk rock Ag:Au ratio is 10, and increases from <3 in central parts of the system towards <10 in peripheral parts of the system (this information is confirmed by a much larger sample population from ore reserve calculations). Positive correlation trends in Cu-Ag, As-Sb, and Hg-Ag plots point to the dominant mineralogical control of these elements by fahlore (Fig. 6). A much weaker positive correlation trend with distinct scatter is displayed by the Cu-Au and Cu-Te variation diagrams which points to the paragenetic relationship of fahlore and gold telluride phases. The Au-Te plot suggests mineralogical control of gold mineralization by tellurides, and the full spectrum of distribution patterns points to synchronous hydrothermal input of the Cu-Au-Ag-Te-As-Sb-Hg element association.

The correlation between this element spectrum is modified by secondary redistribution processes, as seen for very gold-rich and oxidized samples in which native gold is the dominant gold carrier. Such high-gold samples are characterized by low-temperature redistribution and/or supergene enrichment of gold on grain boundaries and fractures with dissolution of fahlore and removal of Cu and Ag (Fig. 6).

Fluorine abundances are generally low in the rocks studied. There was no fluorite seen, and 10 fluorine analyses gave a mean of 185 ppm F (variation range: <150–365 ppm F). The low-F nature of the system is against a hypothetical relationship to hidden alkaline magmatism often associated with Te-rich systems.

Tellurium is relatively immobile in the supergene environment and is not depleted (Fig. 6). Oxidized samples have no Te-bound gold and are 99% cyanide-leachable. The Te component is probably fixed in iron tellurites, known from iron caps over sulfide deposits (Leutwein 1972), or in the abundant jarosite.

Conclusions

Hydrothermal alteration style and mineralogy define the Bereznjakovskoje system as of low-sulfidation (quartz-adularia) epithermal type. This first-order classification is based on the alteration zoning from quartz-sericite/illite ±adularia ±carbonate within veinlets to propylitic assemblages outwards, and the dominant sulfide mineralogy of pyrite and fahlore. Features typical of high-sulfidation systems include high sulfide and copper contents, and gold mineralization associated with tellurides. The association of these features with sericitic alteration, rather than the expected advanced argillic alteration, points to an affiliation with the sulfide-rich variant of low-sulfidation systems, in which fluids intermediate in composition between those responsible for end-member high-and low-sulfidation systems were present. This subtype is typical of a setting in an andesitic terrane at a relatively deep level. On a global scale, sulfide-rich low sulfidation systems appear to be more closely related to porphyry intrusions and to have been generated at greater depths than those with low sulfide contents (Sillitoe 1993). This assumption is supported by the elevated salinity range of 3–8 equivalent wt.% NaCl in fluid inclusions which facilitates base metal transport. The absence of crustiform-banded chalcedony/quartz gangue, so typical for many shallow-seated epithermal systems, and of bladed carbonate-replacement textures indicates that the system is clearly below the hot spring environment and the paleo-boiling level, and suggests potential for subvolcanic porphyry Cu-Au mineralization at depth.

The sulfide-rich low-sulfidation system consists of an early barren pyrite stage followed by a base- and precious metal-rich fahlore-telluride stage. The system is characterized by a distinct Te signature, together with the strongly enriched Au-Sb-As metal spectrum. High Te and relatively high base metal content point to a setting more closely related to intrusive rocks than for sulfide-poor low-sulfidation systems (Sillitoe 1995). The occurrence of several contemporaneous gold-rich copper porphyry showings 10–20 km north from the Bereznjakovskoje prospect is consistent with this assumption (Grabezhev et al. 1995). A similar association between sulfide-rich low-sulfidation gold deposits, volcanoplutonic activity and gold-rich copper porphyries is particularly well known from a number of late Miocene to Quaternary examples in the western Pacific island arcs, especially from the Philippines and Papua New Guinea (Sillitoe 1989).

The Bereznjakovskoje mineralization/alteration trend represents a several kilometer in size system with a number of smaller ore centers. Hydrothermal flow is distributed in small-scale fracture systems over a large area. The dispersed nature of hydrothermal flow makes the ore system difficult to explore and requires a multi-method approach with soil geochemistry and ground geophysics (such as realsection IP) as major tools for drill target selection. The relatively erratic distribution of ore shoots within the extensive vein system allows only part of the mineralization to be defined as mineable ore during the mine development stage, but implies a much larger ore potential.

References

Afifi AM, Kelly WC, Essene EJ (1988) Phase relations among tellurides, sulfides, and oxides: I. Thermochemical data and calculated equilibria. II. Applications to telluride-bearing ore deposits. Econ Geol 83: 377–394, 395–404

Ahmad M, Solomon M, Walshe JL (1987) Mineralogical and geochemical studies of the Emperor gold telluride deposit, Fiji. Econ Geol 82: 345–370

Barton PB Jr, Skinner BJ (1979) Sulfide mineral stabilities. In: Barnes HL (ed) Geochemistry of hydrothermal ore deposits. Wiley, pp 278–403

Benevolski BI (1995) Gold of Russia. Prospects of the use and replacement of mineral resources (in Russian). Roskomnedra/ Geoinformmark, Moscow, 88 p

Berzin R, Oncken O, Knapp JH, Pérez-Estaún A, Hismatulin T, Yunusov N, Lipilin A (1996) Orogenic evolution of the Ural Mountains: results from an integrated seismic experiment. Science 274: 220–221

Dong G, Morrison GW (1995) Adularia in epithermal veins, Queensland: morphology, structural state and origin. Mineral Deposita 30: 11–19

Dong G, Morrison G, Jaireth S (1995) Quartz textures in epithermal veins, Queensland – classification, origin, and implication. Econ Geol 90: 1841–1856

Dowling K, Morrison G (1989) Application of quartz textures to the classification of gold deposits using North Queensland examples. Econ Geol Monogr 6: 342–355

EMJ (1996) Russia. Eng Mining J 197 (11): 18–20

Grabezhev AI, Korobeinikov AF, Moloshag VP (1995) Gold in the copper-gold porphyric deposits of Urals (in Russian). Geokhimija 1995: 1465–1471

Heald P, Foley NK, Hayba DO (1987) Comparative anatomy of volcanic-hosted epithermal deposits: acid sulfate and adularia-sericite types. Econ Geol 82: 1–25

Leutwein F (1972) Tellurium. In: Wedepohl KH (ed) Handbook of geochemistry II/4, Springer, Berlin Heidelberg New York pp 52-B to 52-O

Pearce JA, Harris NBW, Tindle AG (1984) Trace element discrimination diagrams for the tectonic interpretation of granitic rocks. J Petrol 25: 956–983

Pushakov BA, Kuznezov IS (1995) Metasomatism and ore formation in the Bereznjakovskoje gold porphyry deposit (in Russian). Roskomnedra Chelyabinsk, Intern Rep, 48 p

Sengör AMC, Natal'in BA, Burtman VS (1993) Evolution of the Altaid tectonic collage and Paleozoic crustal growth in Eurasia. Nature 364: 299–307

Sibson R (1996) Fluid-generated structural permeability in pre-stressed crust. Ext Abstr Short Course Mesothermal gold deposits: a global overview. Geology Department, University of Western Australia Publication 27: 100–103

Sillitoe RH (1989) Gold deposits in western Pacific island arcs: the magmatic connection. Econ Geol Monogr 6: 274–291

Sillitoe RH (1993) Epithermal models: genetic types, geometrical controls and shallow features. Geol Assoc Canada Spec Pap 40: 403–417

Sillitoe RH (1995) Exploration and discovery of base- and precious-metal deposits in the circum-Pacific region during the last 25 years. Res Geol Spec Iss 19: 1–119

Taylor SR, McLennan SM (1985) The continental crust: its composition and evolution. Blackwell, Oxford, 312 p

Vinogradov AP (1962) Average abundances of chemical elements in major rock types (in Russian). Geokhimija 7: 555–571

Winchester JA, Floyd PA (1977) Geochemical discrimination of different magma series and their differentiation products using immobile elements. Chem Geol 20: 325–343

Zonenshain LP, Korinevsky VG, Kazmin VG, Pechersky DM, Khain VV, Matveenkov VV (1984) Plate tectonic model of the South Urals development. Tectonophysics 109: 95–135